Electromagnetic analysis of a standing-wave dielectric-loaded accelerating structure based on transmission line model

M.Z. Joozdani

*Information and Communication Technology Group, Niroo Research Institute,
Tehran, Iran*

E-mail: mzahir@nri.ac.ir

ABSTRACT: In this paper, a theoretical analysis of a standing-wave dielectric-loaded accelerator based on transmission line model is performed. A practical X-band accelerating structure consisting of a uniform dielectric-loaded tube and a matching cell is considered. The structure is designed to inject high power and long-length radio frequency (RF) pulse into the dielectric-loaded tube at 11.42 GHz. The dominant propagating mode is circular TM_{01} mode accelerating the electron beam along the axis of the structure. Therefore, the kinetic energy of the electron beam is dependent on the longitudinal profile of the axial electric field which can be approximately calculated by the transmission line model. In this method, every uniform part is considered as a transmission line with its own wave number and characteristic impedance. The accelerating structure is analyzed by the proposed method and the axial electric field along the structure and input reflection coefficient are extracted and compared with the simulation result obtained by full-wave electromagnetic (EM) software. It is demonstrated that there is a good agreement between the simulation and analytical results.

Contents

1 Introduction

Dielectric-loaded accelerating (DLA) structures proposed in the early 1950s have been investigated both theoretically and experimentally in the past decades [1]–[6]. Their benefits such as lightweight, compactness, and simplicity of fabrication make them promising alternatives to heavy and bulky metal disk-loaded structures in the development of future high-gradient accelerators. In dielectric wakefield accelerators, high gradients of 5.5 GV/m at terahertz frequencies and 100 MV/m at 10 GHz have been reported when pulse widths are about a few nanoseconds [7, 8]. By coupling external high-power RF to the DLA, a much larger pulse width can be achieved. However, the effects of strong multipactor loading and RF breakdown limit the performance of the DLAs at gradients more than 10 MV/m [9, 10].

Until now, different techniques have been applied to reduce the effects of multipactoring and RF breakdown. It is demonstrated that RF breakdowns have mostly existed at the joints between separate dielectric parts of the tube and coupler or between the tube and its metal jacket. Therefore, some gap-free structures have been proposed to suppress its occurrence [10]–[12]. Additionally, it is shown that fabricating a dielectric tube from materials with a low secondary electron emission coefficient such as quartz can decrease multipactoring. Also, multipactor loading can be decreased about 20% by TiN coating of the interior surface of the dielectric tube applied with physical vapor deposition (PVD) or atomic layer deposition (ALD) [12]. Recently, a new approach using the axial magnetic field of solenoid has been suggested to completely eliminate the single-surface resonant multipactor [13]. This method is performed for both traveling and standing-wave accelerators [14, 15]. Because of the powerful axial and tangential electric fields of the dominant mode in DLA structures, the regime of the multipactor differs from that of the conventional one

happening in RF windows. Thus, new models have been introduced to predict the behavior of this phenomenon [16]–[19].

After solving the multipactoring and breakdown problems, the major challenge behind the fabrication of DLA structures is the proper coupling of high-power RF into the dielectric tube. To date, a variety of couplers have been designed for this purpose [20, 21]. Before the high power test, cold tests are performed to extract the profile of EM fields along the accelerator and scattering matrix parameters of the structure for comparison with simulation and theoretical results. In order to simulate the interaction of beam and microwave, time-domain solvers such as Particle-in-Cell (PIC) are useful for traveling-wave accelerators. However, full-wave EM simulation in the time domain will be very time-consuming and inaccurate for standing-wave accelerating structures. As an approximate solution by neglecting the beam loading effect, the EM fields can be found in frequency-domain solver and imported in the time-domain simulator. This process can also be performed more rapidly by theoretical methods.

A well-known and precise theoretical method, especially for multilayer structures consisting of homogeneous slabs or impedance surfaces, is the transmission line method in which every uniform part is modeled by a transmission line with its own characteristic impedance and propagation constant [22]–[25]. Unfortunately, because of the non-homogeneity of the dielectric-loaded tube and non-uniformity of the RF coupler, this method is not applicable in DLA structures. However, it is shown in this paper that by considering some approximations, the physics of the problem allows us to employ the transmission line model for the structure. An approximation based on power flow is used to calculate the characteristic impedance of the dielectric-loaded tube of the DLA structure. Additionally, higher order modes produced by discontinuities along the structure are neglected and only the dominant mode is considered. Using other methods including higher order modes such as Mode Matching Technique (MMT) for this problem may improve the accuracy a little but increases the complexity of the solution and the time required to reach the answer. However, the simple proposed method has acceptable accuracy and can be easily used for multisection DLAs and non-uniform dielectric-loaded couplers.

In order to perform the transmission line analysis for standing-wave accelerators, a DLA structure fabricated and tested by Jing et al. [20] with some simplifications in the geometrical design is assumed. In section 2, this structure is simulated by an EM full-wave software, and input reflection coefficient and axial electric field magnitude along the structure are extracted. In section 3, the DLA structure and RF coupler are divided into six uniform parts and every part is modeled by a transmission line. Therefore, the accelerator can be modeled by a series of transmission lines with a boundary condition at the end of the structure. The analytical results obtained by proposed method are compared with the simulation results in section 4, and it is shown that there is a good agreement between them. It is also explained how this method can be used in a fast optimization process to find an approximate initial point for more accurate full-wave optimizations. Finally, conclusions are made in section 5.

## 2 A practical dielectric-loaded accelerating structure

As shown in figure 1, the accelerator consists of an RF coupler and a dielectric-loaded structure which are covered by a metallic body not depicted in this figure. For the sake of simplicity,
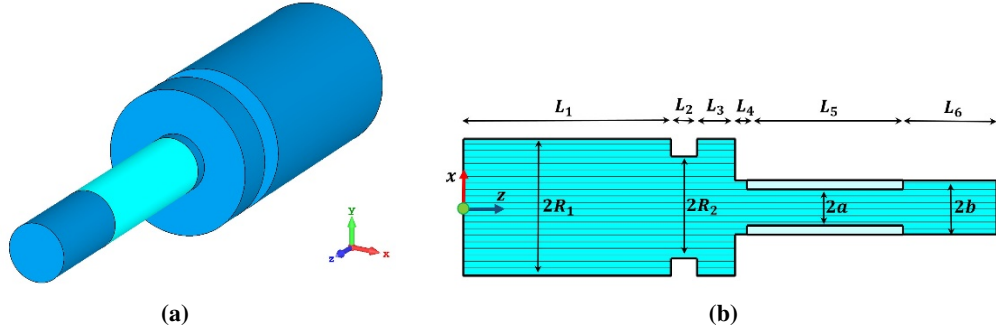
Figure 1. Accelerator structure (a) perspective view, (b) cross-sectional view and dimensional parameters.

the metallic body is assumed to be a perfect electric conductor (PEC) and curved edges at the discontinuities of the structure are considered to be sharp. It should be noted that these assumptions cannot limit the proposed theoretical method.

The dielectric tube is made of MCT20 with the permittivity of $\varepsilon_r = 20$ and loss tangent of $\tan \delta = 1 \times 10^{-4}$. The inner and outer radii of the dielectric tube are $a = 3\,\text{mm}$ and $b = 4.567\,\text{mm}$, respectively. Other structural parameters are as follows: $L_1 = 34.4\,\text{mm}$, $L_2 = 4.3\,\text{mm}$, $L_3 = 6.3\,\text{mm}$, $L_4 = 2\,\text{mm}$, $L_5 = 25.8\,\text{mm}$, $L_6 = 15.5\,\text{mm}$, $R_1 = 11.47\,\text{mm}$, and $R_2 = 8.6\,\text{mm}$.
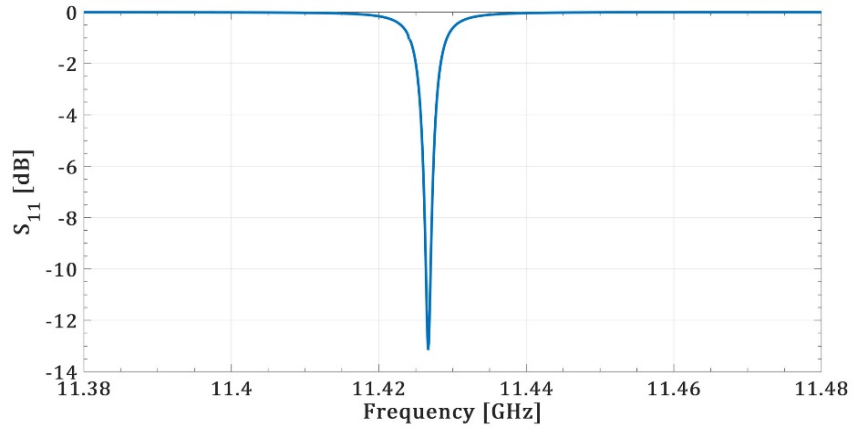

Figure 2. Reflection coefficient from the input of the accelerator.

This structure is simulated by the frequency-domain solver of Computer Simulation Technology (CST) Studio software in which the maximum input power of 1 W is selected by default. The dominant mode of the structure is TM01 and the coupler matches the dielectric-loaded structure to the RF source. Reflection response from the input of the structure is illustrated in figure 2. Evidently, the minimum of reflection magnitude is −13.1 dB at the frequency of 11.4267 GHz and the bandwidth of reflection below −10 dB is about 0.5 MHz which is very narrow. The axial electric field magnitude along the axis of the structure is plotted in figure 3. Also, the cross-sectional view of its distribution in the accelerator structure is depicted in figure 4. The origin of the coordinate system is at the center of the coupler input. Figures 3 and 4 are both obtained at the center frequency of $f = 11.4267\,\text{GHz}$. Moreover, the maximum amplitude of the axial electric field is in the dielectric
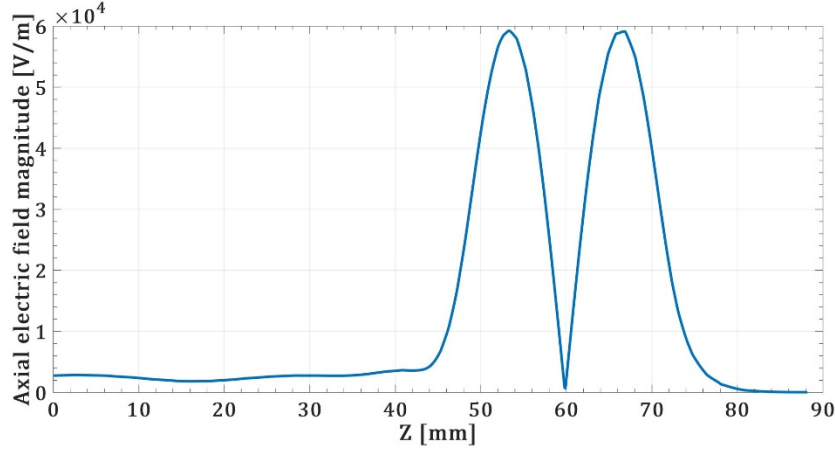
Figure 3. Axial electric field magnitude along the axis of the accelerator structure at $f = 11.4267\,\text{GHz}$.
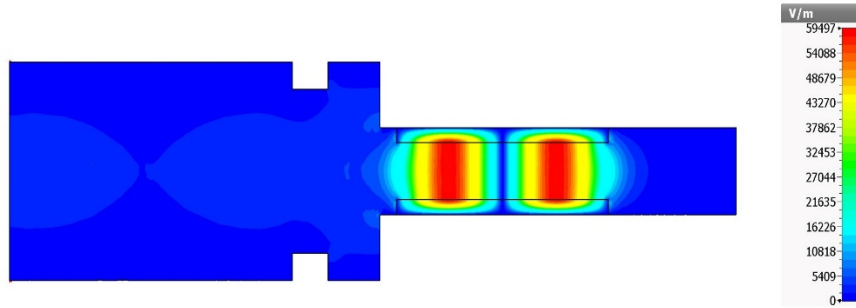
Figure 4. Distribution of axial electric field magnitude in the accelerator structure at $f = 11.4267\,\text{GHz}$.

tube with two peaks of about 6×10^4 V/m at the maximum input power of 1 W. Thus, by increasing the power to 10 MW, the gradient of 180 MV/m can be achieved.

3 Transmission line model analysis of the accelerator

Based on figure 1 the accelerator structure can be divided into six parts with lengths of L_1 to L_6. Each part can be modeled by a transmission line with its propagation constant and characteristic impedance. In the following subsections, propagation constant and characteristic impedance of conventional and dielectric-loaded waveguides are discussed, and the reflection of the accelerator structure and field distribution along the axis of the accelerator are formulized.

3.1 Propagation constant and characteristic impedance of conventional cylindrical waveguides

In conventional cylindrical waveguide with a PEC wall, the propagation constant in the axial direction for TM_{01} mode can be calculated as:

$$\gamma = \sqrt{\left(\frac{\chi_{01}}{R_i}\right)^2 - k_0^2} \tag{3.1}$$

in which k_0, χ_{01}, and R_i are propagation constant in free space, first root of Bessel function of the first kind of zero order, and radius of the waveguide of the ith section, respectively. According to the value of R_i, the propagation constant can be completely imaginary or real at a constant frequency. Thus, at the working frequency, for the first and third sections of the accelerator, γ is completely imaginary and TM_{01} is the propagating mode. On the other hand, for the second, fourth, and sixth sections, γ is completely real and TM_{01} is an evanescent mode. On the other hand, for the fourth and sixth sections, γ is completely real and TM_{01} is an evanescent mode. The characteristic impedance for the TM mode wave is:

$$Z_c = \frac{-j\gamma}{\omega\varepsilon_0} \,. \tag{3.2}$$

3.2 Propagation constant and characteristic impedance of dielectric-loaded cylindrical waveguides

In dielectric-loaded waveguides, TM modes have three components of E_r, H_ϕ, and E_z. Using boundary conditions at inner and outer radii of the dielectric tube, the characteristic equation can be obtained as [1]:

$$\frac{\varepsilon_0}{k_1 a} \frac{J_0{}'(k_1 a)}{J_0(k_1 a)} - \frac{\varepsilon_0 \varepsilon_r}{k_2 a} \frac{F_{00}{}'(k_2 a)}{F_{00}(k_2 a)} = 0 \tag{3.3}$$

in which k_1 and k_2 are radial components of propagation constant in vacuum and the dielectric tube, respectively. In addition, F_{00} and F_{00}' are functions defined as follows:

$$F_{00}(k_2 r) = J_0(k_2 r) - \frac{J_0(k_2 b)}{Y_0(k_2 b)} Y_0(k_2 r) \tag{3.4}$$

$$F_{00}{}'(k_2 r) = J_0{}'(k_2 r) - \frac{J_0(k_2 b)}{Y_0(k_2 b)} Y_0{}'(k_2 r) \,. \tag{3.5}$$

Because of dielectric loss, the propagation constant in the axial direction in the dielectric tube is a complex value and can be calculated as:

$$\gamma = \alpha + j\beta \tag{3.6}$$

where α and β are attenuation and phase constants, in that order. Considering a dielectric tube with the inner radius of $a = 3$ mm and outer radius of $b = 4.567$ mm, attenuation and phase constants are calculated and plotted in figures 5 and 6, respectively. It is clear that dispersion characteristics of only the first three TM modes are demonstrated in the frequency range from zero to 50 GHz and the cut-off frequencies of other higher order TM modes are above 50 GHz. Using theses plots, α and β can be obtained at the working frequency of the accelerating structure. It is noteworthy that in the proposed method, due to the powerful coupling between the axial electric field of TM_{01} mode in the coupler and the dielectric tube, the excitation of TE and HE modes are neglected.

Characteristic impedance of TM_{01} mode is different in the vacuum and dielectric parts of the dielectric-loaded waveguide. However, characteristic impedances of the dielectric and vacuum parts can be combined to calculate an average value for characteristic impedance of the dielectric-loaded waveguide as $Z_c = \frac{-j\gamma}{\omega\varepsilon_0}(\eta/\varepsilon_r + 1 - \eta)$ in which η is the ratio of power flow in the dielectric part to the total power flow in the dielectric-loaded waveguide. For the studied case $\eta \approx 0.9$ in the frequency range of 11.3 GHz to 11.5 GHz.
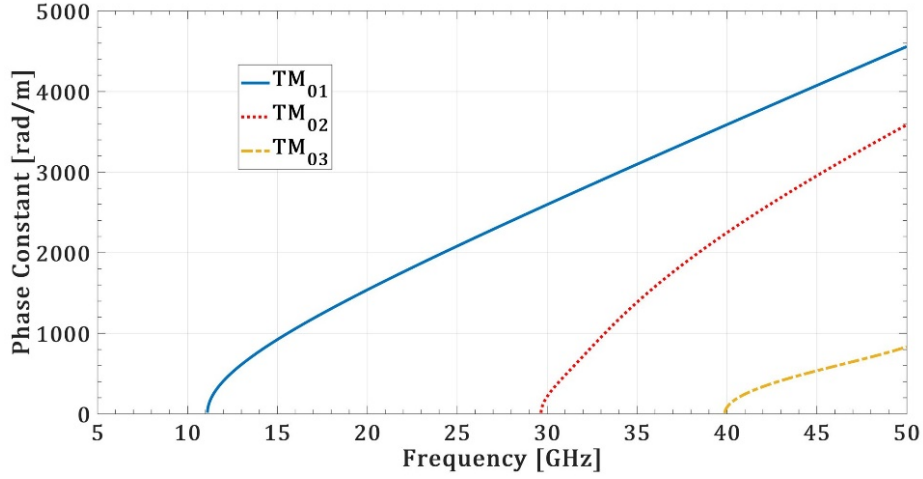
Figure 5. Phase constant of TM modes in the frequency range from zero to 50 GHz.
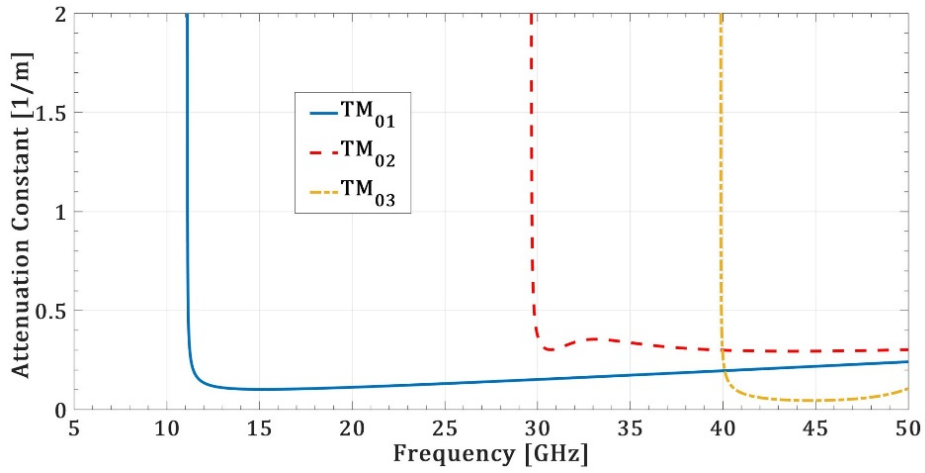
Figure 6. Attenuation constant of TM modes in the frequency range from zero to 50 GHz.

3.3 Calculation of the input reflection and axial electric field distribution along the accelerator

The transmission line model is an essential and quick solution for waveguides with a fixed cross-section, fully or partially filled with non-homogeneity in the propagation direction. Nevertheless, the acceleration structure has non- uniformity in the coupler and non-homogeneity in the dielectric-loaded tube in the radial direction. Therefore, it seems that the use of the transmission line method is not applicable in this problem. On the other hand, only the calculation of electric field on and closely around the axis of the structure is important for finding the acceleration force on the electron beam. Thus, using the approximation explained in the section 3.2 to calculate the characteristic impedance of dielectric-loaded tube and continuity of electric field on the axis of the structure, make this method applicable to obtain a rapid and close approximation to time-consuming full-wave simulation.

To investigate the analysis of the accelerating structure with the transmission line model, the whole structure is divided into six sections. Every part is modeled by a transmission line with its

own propagation constant and characteristic impedance. Transmission matrix of each section can be defined as:

$$T_i = \begin{bmatrix} \cosh\left(\gamma_i l_i/2\right) & Z_{c,i} \sinh\left(\gamma_i l_i/2\right) \\ Z_{c,i}^{-1} \sinh\left(\gamma_i l_i/2\right) & \cosh\left(\gamma_i l_i/2\right) \end{bmatrix} \tag{3.7}$$

in which γ_i, $Z_{c,i}$, and l_i are propagation constant, characteristic impedance, and length of the ith section, in that order. The total transmission matrix of the accelerating structure can be calculated as:

$$T = \begin{bmatrix} A & B \\ C & D \end{bmatrix} = \prod_{i=1}^{6} T_i \,. \tag{3.8}$$

The accelerating structure can be considered as a series of transmission lines with a short circuit at the end of the structure. The reflection coefficient of the input port can be achieved from the total transmission matrix parameters as:

$$\Gamma_{\text{in}} = \frac{B - Z_{c,1}D}{B + Z_{c,1}D} \,. \tag{3.9}$$

Axial electric field (E_z) along the accelerating structure is a standing-wave consisting of incident and reflection waves in every section which can be written as:

$$E_{z,i} = E_i \left(e^{-\gamma_i z} + \Gamma_i e^{\gamma_i z} \right) \tag{3.10}$$

where E_i and Γ_i are the amplitude of incident axial electric field and reflection coefficient in the ith section, respectively. Reflection coefficient in the ith section can be defined as:

$$\Gamma_i = \frac{Z_{l,i} - Z_{c,i}}{Z_{l,i} + Z_{c,i}} \tag{3.11}$$

where $Z_{l,i}$ is the load impedance at the end of ith section which is equal to the input impedance of the next section. Also, there is a recurrence relation between the load impedances as:

$$Z_{l,i-1} = Z_{c,i} \frac{Z_{l,i} + Z_{c,i} \tanh\left(\gamma_i l_i\right)}{Z_{c,i} + Z_{l,i} \tanh\left(\gamma_i l_i\right)} \,. \tag{3.12}$$

By considering $Z_{l,6} = 0$ and $\Gamma_6 = -1$ and performing mathematical calculations in (3.11) and (3.12), the reflection coefficient for all of the sections can be achieved. Also, using the continuity of electric field E_z on the axis of the structure at the boundary of adjacent sections, E_z distribution on the axis can be written corresponding to one unknown variable (E_5). To determine this variable, dissipated power is used which can be calculated as:

$$P_{\text{diss}} = P_{\text{in}} \left(1 - |\Gamma_{\text{in}}|^2 \right) \tag{3.13}$$

in which P_{in} is the input power. As the walls of the accelerator are assumed to be PEC, all of the inserted power is dissipated in the dielectric part of the structure. According to the electromagnetic fields in the dielectric-loaded tube, power loss can be rewritten as:

$$P_{\text{diss}} = \int_a^b \int_0^{2\pi} \int_0^{l_5} \frac{1}{2} \omega \varepsilon_0 \varepsilon_r \tan \delta \, |E|^2 \, r \, dr \, d\varphi \, dz \,. \tag{3.14}$$

To calculate (3.14), axial and radial electric field of TM_{01} mode in the dielectric-loaded tube are required which can be considered as:

$$E_z \begin{cases} E_{z,5} = E_5 \, J_0 \, (k_1 r) \, 0 \le r \le a \\ E_{z,5} = E_5 \, \frac{J_0(k_1 a)}{F_{00}(k_2 a)} F_{00} \, (k_2 r) \, a \le r \le b \end{cases} \tag{3.15a}$$

$$E_r \begin{cases} E_{r,5} = E_5 \frac{-\gamma_5}{k_1} \, J_0{}' \, (k_1 r) \, 0 \le r \le a \\ E_{r,5} = E_5 \frac{-\gamma_5}{k_2} \, \frac{J_0(k_1 a)}{F_{00}(k_2 a)} F_{00}{}' \, (k_2 r) \, a \le r \le b \end{cases} \tag{3.15b}$$

where all of the fields have an $e^{-\gamma_5 z} + \Gamma_5 e^{\gamma_5 z}$ term which is not written for the sake of simplicity. By substituting E_z and E_r at $a \le r \le b$ in (3.14) and setting it equal to (3.13), E_5 and axial electric field amplitude in other sections can be obtained. Thus, the axial electric field profile along the axis of the structure can be plotted.

4   Analytical results and comparison with simulation results

In this section the DLA structure introduced and studied by the full-wave simulation in section 2 is analyzed by the proposed method, and the analytical results are compared with the simulated ones. First, the reflection coefficient from the input of the structure is obtained and plotted in figure 7. It is observed that the minimum of the reflection is -15 dB occurring at $f = 11.42$ GHz. Thus, there is an about 6.7 MHz shift in working frequency which means a 0.06% error relative to the simulation result. The frequency shift and increase in minimum reflection value are due to the approximations assumed in the proposed method, including the purity of one electromagnetic mode in the accelerating structure in spite of discontinuities along the structure and the characteristic impedance value for the dielectric-loaded tube.

As the working bandwidth of the structure is very narrow compared with working frequency, the working bandwidth obtained by the proposed method has nothing in common with the simulated bandwidth. Frequency shifting is usually observed in the accelerating structures after fabrication and such little frequency shift does not pose a problem for the wideband sources. However, it is important that the axial electric field in the structure should have the desired profile in the working frequency. In figure 8, the axial electric field magnitude along the structure is plotted and compared with the simulation result. Although the simulated and analytical electric field profiles are obtained at different frequencies, they are in good agreement with each other, particularly in the dielectric-loaded tube. The most important part of the structure accelerating the electron beam is the dielectric-loaded tube in which the electric field magnitude is much larger than elsewhere. Therefore, to calculate the electron beam energy, only the electric field in the dielectric-loaded tube can be considered.

By knowing the axial electric field profile along the structure, the initial value of beam energy, and input power magnitude, electron beam energy can be quickly found along the structure. If some ranges are determined for the working frequency and energy of accelerated beam at the end of the structure, optimization methods such as Genetic Algorithm can be employed to find the structural variables to reach these goals. However, due to the little frequency shift and difference in reflection amplitudes, more accurate full-wave simulation and fine changes in structural variables
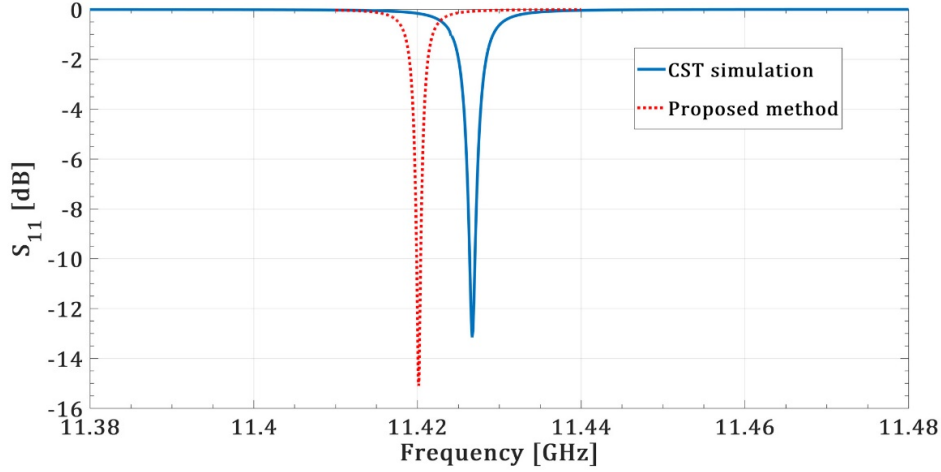
Figure 7. Reflection coefficient from the input of the accelerating structure obtained by the proposed method and full-wave simulation.
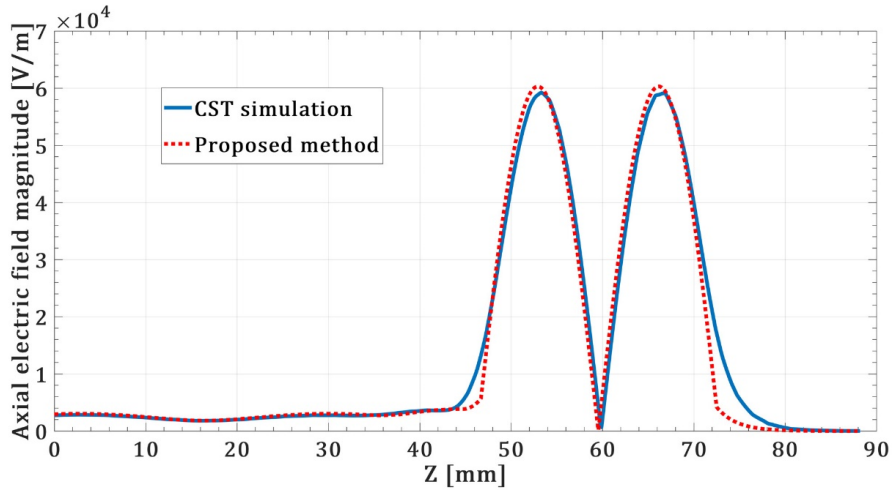
Figure 8. Comparison of the axial electric field magnitude along the axis of the structure between CST simulation at f=11.4267 GHz and the proposed method at f=11.42 GHz.

are required to finalize the design. Consequently, the output values of the variables extracted by the combination of the proposed method and optimization can be utilized as an initial point for the optimization of the structure by full-wave simulation, thus significantly reducing the total time of full-wave optimization.

5 Conclusion

In this paper, an approximation analysis based on the transmission line model is proposed for a practical DLA structure consisting of a coupler and uniform dielectric-loaded tube. As the electron beam accelerated around the axis of the structure, the kinetic energy of the electron beam at the end of the accelerator depends mostly on the axial electric field along the structure. In this case, the proposed method can estimate the working frequency and axial electric field profile in the dielectric-

loaded tube with good accuracy in comparison with simulation results. Due to the high coupling between the coupler and DLA, only fundamental mode is accounted making the proposed method fast and simple. Additionally, it can be easily performed for multi-section DLAs and dielectric-loaded couplers in which considering higher order modes makes the problem complicated and time-consuming. Also, it is discussed that this analytical method with the combination of optimization processing such as GA can provide a fast solution for initial design parameters. Then, more accurate full-wave optimizations can use them as initial point to reduce the whole time of optimization.

References

[1] G.T. Flesher and G.I. Cohn, *Dielectric loading for waveguide linear accelerators*, *Trans. Am. Inst. Electr. Eng.* **70** (1951) 887.

[2] R.B. R.-Shersby-Harvie, L. Mullett, W. Walkinshaw, J. Bell and B. Loach, *A theoretical and experimental investigation of anisotropic-dielectric-loaded linear electron accelerators*, *Proc. IEE* **B 104** (1957) 273.

[3] P. Zou, W. Gai, R. Konecny, X. Sun, T. Wong and A. Kanareykin, *Construction and testing of an* 11.4 *GHz dielectric structure based traveling wave accelerator*, *Rev. Sci. Instrum.* **71** (2000) 2301.

[4] C. Jing, A. Kanareykin and S. Kazakov, *Development of dual layered dielectric-loaded accelerating structure*, in proceedings of the *2007 IEEE Particle Accelerator Conference (PAC)*, Albuquerque, NM, U.S.A., 25–29 June 2007.

[5] C. Jing, W. Liu, W. Gai, J. Power and A. Kanareykin, 34.272 *GHz multilayered dielectric-loaded accelerating structure*, in proceedings of the *2005 Particle Accelerator Conference*, Knoxville, TN, U.S.A., 16–20 May 2005.

[6] A. Kanareykin, W. Gai, E. Nenasheva, S. Karmanenko and I. Sheinman, *A method for tuning dielectric loaded accelerating structures*, in proceedings of the *2003 Bipolar/BiCMOS Circuits and Technology Meeting (IEEE Cat. No. 03CH37440)* Portland, OR, U.S.A., 12–16 May 2003.

[7] M.C. Thompson et al., *Breakdown Limits on Gigavolt-per-Meter Electron-Beam-Driven Wakefields in Dielectric Structures*, *Phys. Rev. Lett.* **100** (2008) 214801.

[8] M.E. Conde, *Survey of advanced dielectric wakefield accelerators*, in proceedings of the *2007 IEEE Particle Accelerator Conference (PAC)*, Albuquerque, NM, U.S.A., 25–29 June 2007.

[9] J.G. Power et al., *Observation of multipactor in an alumina-based dielectric-loaded accelerating structure*, *Phys. Rev. Lett.* **92** (2004) 164801.

[10] C. Jing et al., *High-power RF tests on X-band external powered dielectric-loaded accelerating structures*, *IEEE Trans. Plasma Sci.* **33** (2005) 1155.

[11] C. Jing, A. Kanareykin, R. Konecny, J.G. Power, S.H. Gold and S. Kazakov, *Progress towards a gap free dielectric-loaded accelerator*, in proceedings of the *2007 IEEE Particle Accelerator Conference (PAC)*, Albuquerque, NM, U.S.A., 25–29 June 2007.

[12] C. Jing et al., *Progress toward externally powered X-band dielectric-loaded accelerating structures*, *IEEE Trans. Plasma Sci.* **38** (2010) 1354.

[13] C. Chang, J. Verboncoeur, S. Tantawi and C. Jing, *The effects of magnetic field on single-surface resonant multipactor*, *J. Appl. Phys.* **110** (2011) 063304.

[14] C. Jing et al., *Observation of multipactor suppression in a dielectric-loaded accelerating structure using an applied axial magnetic field*, *Appl. Phys. Lett.* **103** (2013) 213503.

[15] C. Jing, S.H. Gold, R. Fischer and W. Gai, *Complete multipactor suppression in an X-band dielectric-loaded accelerating structure*, *Appl. Phys. Lett.* **108** (2016) 193501.

[16] J.G. Power and S.H. Gold, *Multipactor modeling in cylindrical dielectric-loaded accelerators*, *AIP Conf. Proc.* **877** (2006) 362.

[17] L. Wu and L.K. Ang, *Multipactor discharge in a dielectric-loaded accelerating structure*, *Phys. Plasmas* **14** (2007) 013105.

[18] O.V. Sinitsyn, G.S. Nusinovich and T.M. Antonsen Jr., *Self-consistent nonstationary two-dimensional model of multipactor in dielectric-loaded accelerator structures*, *Phys. Plasmas* **16** (2009) 073102.

[19] O.V. Sinitsyn, G.S. Nusinovich and T.M. Antonsen Jr., 3*D Monte-Carlo simulations of multipactor in dielectric-loaded accelerating structures*, *AIP Conf. Proc.* **1507** (2012) 505.

[20] C. Jing et al., *An X-band standing wave dielectric loaded accelerating structure*, in proceedings of the *3rd International Particle Accelerator Conference (IPAC 2012)*, New Orleans, Louisiana, U.S.A., 20–25 May 2012 [*Conf. Proc.* **C 1205201** (2012) 1927].

[21] W. Liu and W. Gai, *Design of dielectric accelerator using TE-TM mode converter*, *AIP Conf. Proc.* **647** (2002) 469.

[22] M.Z. Joozdani, M.K. Amirhosseini and A. Abdolali, *Equivalent circuit model for frequency-selective surfaces embedded within a thick plasma layer*, *IEEE Trans. Plasma Sci.* **43** (2015) 3590.

[23] M.Z. Joozdani and M.K. Amirhosseini, *Equivalent circuit model for the frequency-selective surface embedded in a layer with constant conductivity*, *IEEE Trans. Antennas Propag.* **65** (2017) 705.

[24] M.Z. Joozdani and M.K. Amirhosseini, *Wideband absorber with combination of plasma and resistive frequency selective surface*, *IEEE Trans. Plasma Sci.* **44** (2016) 3254.

[25] M.Z. Joozdani and M.K. Amirhosseini, *Equivalent circuit model for frequency selective surfaces embedded within magnetic layer*, in proceedings of the *7th International Symposium on Telecommunications (IST'2014)*, Tehran, Iran, 9–11 September 2014.